


 Cite this: *Chem. Commun.*, 2014, 50, 11591

 Received 8th May 2014,
 Accepted 6th August 2014

DOI: 10.1039/c4cc03487b

www.rsc.org/chemcomm

A hybrid polyoxometalate–organic molecular catalyst for visible light driven water oxidation†

 C. Zhang,^a X. Lin,^a Z. Zhang,^{ab} L.-S. Long,^c C. Wang^b and W. Lin^{*abc}

A novel organic–inorganic hybrid monocapped/bicapped Keggin structure $[\text{Co}^{\text{II}}(\text{bpy})_3]_6(\text{H}_2\text{bpy})[(\text{Co}^{\text{II}}\text{bpy})_2(\text{PMo}_8^{\text{VI}}\text{Mo}_4^{\text{VO}}\text{O}_{40})]_3 [(\text{Co}^{\text{II}}\text{bpy})-(\text{PMo}_8^{\text{VI}}\text{Mo}_4^{\text{VO}}\text{O}_{40})] \cdot 16\text{H}_2\text{O}$ (bpy = 2,2'-bipyridine) was synthesized and shown to be an efficient visible light-driven catalyst for water oxidation.

The rising global energy demand and increasing adverse environmental impacts of fossil fuel consumption represent a daunting societal challenge.¹ To address this challenge, scientists have striven to develop clean and renewable energy resources, among which solar energy is a promising candidate.² The development of scalable technology to efficiently convert solar energy to chemical fuels (*e.g.*, photocatalytic splitting of water to hydrogen and oxygen) will meet the future energy needs without environmental consequences. As a result, water oxidation, a critical step in converting sunlight to chemical energies, has received increasing attention in the past few decades.³ Significant efforts have recently been devoted to the discovery of water oxidation catalysts (WOCs) based on earth abundant elements in order to enable economical and scalable production of solar fuels.^{4,5} The design of molecular WOCs presents a significant challenge due to the highly oxidative nature of the active WOC and the reaction environment. Among the organic ligands examined, 2,2'-bipyridine (bpy) is the most established ligand for synthesizing molecular WOCs owing to its oxidative stability.⁶ On the other hand, polyoxometalates (POMs), a subset of metal–oxo clusters with oxygen-enriched surfaces,⁷ have also been investigated as oxidatively stable ligands for

designing active WOCs in the past few years.^{3i,8} The tetranuclear Co-based POM $[\text{Co}_4(\text{H}_2\text{O})_2(\text{PW}_9\text{O}_{34})_2]^{10-}$ was, for example, demonstrated as an efficient homogeneous catalyst in visible-light-driven water oxidation using $[\text{Ru}(\text{bpy})_3]^{2+}$ as the photosensitizer and $\text{Na}_2\text{S}_2\text{O}_8$ as the sacrificial electron acceptor.^{9–11} A number of other Co- and Ni-based POM WOCs have recently been used for visible-light-driven water oxidation reactions.^{8b,d,10,12} As Keggin-type POMs are the most stable structures in POM chemistry,¹³ we aimed to design Co-based POMs of Keggin-type structures for water oxidation. Herein we wish to report the synthesis and characterization of a novel organic–inorganic hybrid monocapped/bicapped Keggin structure $[\text{Co}^{\text{II}}(\text{bpy})_3]_6(\text{H}_2\text{bpy})[(\text{Co}^{\text{II}}\text{bpy})_2(\text{PMo}_8^{\text{VI}}\text{Mo}_4^{\text{VO}}\text{O}_{40})]_3 [(\text{Co}^{\text{II}}\text{bpy})(\text{PMo}_8^{\text{VI}}\text{Mo}_4^{\text{VO}}\text{O}_{40})] \cdot 16\text{H}_2\text{O}$, **1**, and its use as an efficient visible light-driven catalyst for water oxidation. In this strategy, we combine the well-established bpy ligand with stable Keggin-type POMs to design robust organic–inorganic hybrid molecular WOCs.

1 was synthesized hydrothermally by heating a mixture of Na_2MoO_4 , $\text{Co}(\text{Ac})_2$, 2,2'-bpy, 4,4'-bis(phosphonomethyl)biphenyl, Na_2HPO_4 , and a small amount of 85% H_3PO_4 in water. Single-crystal X-ray diffraction studies revealed that **1** crystallizes in the monoclinic space group $P2_1/c$ (Table S1, ESI†). Each asymmetric unit of **1** consists of two crystallographically distinct POM anions: one $[(\text{Co}^{\text{II}}\text{bpy})_2(\text{PMo}_8^{\text{VI}}\text{Mo}_4^{\text{VO}}\text{O}_{40})]^{3-}$ and one unit formally denoted as $[(\text{Co}^{\text{II}}\text{bpy})_{1.5}(\text{PMo}_8^{\text{VI}}\text{Mo}_4^{\text{VO}}\text{O}_{40})]^{4-}$ (Fig. 1). The latter unit results from an average of a 50:50 occupancy disorder of one bicapped Keggin $[(\text{Co}^{\text{II}}\text{bpy})_2(\text{PMo}_8^{\text{VI}}\text{Mo}_4^{\text{VO}}\text{O}_{40})]^{3-}$ and one monocapped $[(\text{Co}^{\text{II}}\text{bpy})(\text{PMo}_8^{\text{VI}}\text{Mo}_4^{\text{VO}}\text{O}_{40})]^{5-}$. The 0.5 $(\text{Co}^{\text{II}}\text{bpy})$ units in the latter POM anion reside at the inversion center, which crystallographically relates the bicapped and monocapped Keggin structures and introduces the occupancy disorder. There are thus three bicapped Keggin structures and one monocapped Keggin structure in the formula unit of **1**. In **1**, the charge is balanced by six $[\text{Co}^{\text{II}}(\text{bpy})_3]^{2+}$ and one protonated bpy as counter cations in the asymmetric unit.

Bond valence sum (BVS, Table S2 in ESI†) calculations¹⁴ gave an average valence of 5.67 for all 24 Mo atoms, corresponding to the expected valence of 5.66 for $\text{Mo}^{\text{V}}_{16}\text{Mo}^{\text{VI}}_{32}$. On the other hand, BVS calculations confirmed that all cobalt atoms are in

^a Collaborative Innovation Center of Chemistry for Energy Materials, College of Chemistry and Chemical Engineering, Xiamen University, Xiamen 361005, P. R. China

^b Department of Chemistry, University of Chicago, 929 E 57th Street, Chicago, IL 60637, USA. E-mail: wenbinlin@uchicago.edu

^c State Key Laboratory of Physical Chemistry of Solid Surfaces, Department of Chemistry, College of Chemistry and Chemical Engineering, Xiamen University, Xiamen 361005, P. R. China

† Electronic supplementary information (ESI) available: Experimental details, X-ray crystallography, BVS calculations, XPS spectra, TG curves, CV curves, DLS spectrum and IR spectra. CCDC 999859. For ESI and crystallographic data in CIF or other electronic format see DOI: 10.1039/c4cc03487b

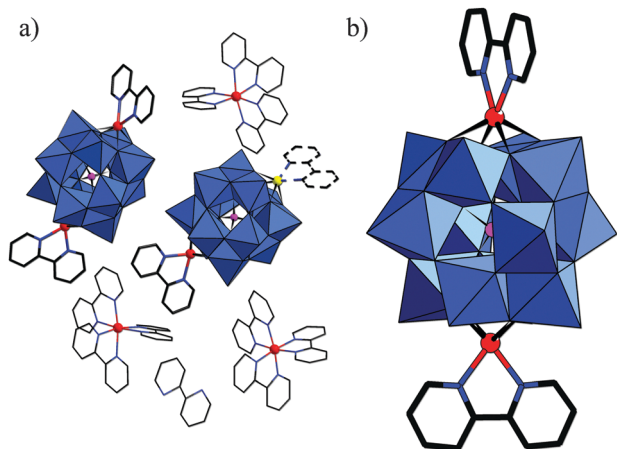
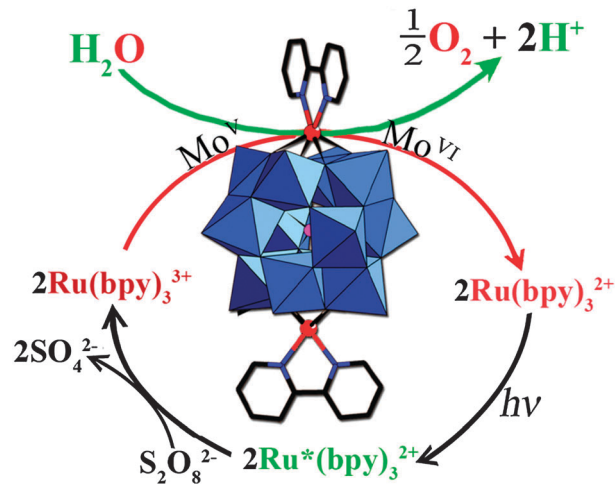


Fig. 1 (a) The asymmetric unit of **1** contains one $[(\text{Co}^{\text{II}}\text{bpy})_2(\text{PMo}_8^{\text{VI}}\text{Mo}_4^{\text{V}}\text{O}_{40})]^{3-}$ unit and one $[(\text{Co}^{\text{II}}\text{bpy})_{1.5}(\text{PMo}_8^{\text{VI}}\text{Mo}_4^{\text{V}}\text{O}_{40})]^{4-}$ unit along with three $\text{Co}^{\text{II}}(\text{bpy})_3$ and one H_2bpy cations. (b) The biccapped Keggin structure shows coordination of the $\text{Co}^{\text{II}}\text{bpy}$ unit to four terminal oxygen atoms of the POM. All of the hydrogen atoms and lattice water molecules have been omitted for clarity. Colour code: blue polyhedra: Mo; red ball: Co; yellow ball: disordered Co; violet: P; black: C; and blue: N. The disordered $\text{Co}^{\text{II}}(\text{bpy})$ subunit is shown with dotted lines.

the +2 oxidation state. The assignments of oxidation states are confirmed by X-ray photoelectron spectroscopy (XPS) measurements (Fig. S1, ESI†). Four deconvoluted peaks were observed in the Mo 3d region at 231.39, 232.51, 234.30, and 235.55 eV, attributed to $\text{Mo}^{\text{V}} 3d_{5/2}$, $\text{Mo}^{\text{VI}} 3d_{5/2}$, $\text{Mo}^{\text{V}} 3d_{3/2}$, and $\text{Mo}^{\text{VI}} 3d_{3/2}$ respectively.¹⁵ The binding energy values of Co atoms in **1** at the 2p region are 780.90, 786.85, 796.80 and 803.00 eV, corresponding to $\text{Co}^{\text{II}} 2P_{3/2}$, $\text{Co}^{\text{II}} 2P_{1/2}$ and their respective satellite peaks.¹⁶ Thermal gravimetric analysis (TGA) indicates a weight loss of 2.35% in the range of 25–350 °C, attributed to the removal of about 16 crystal water molecules (Fig. S2, ESI†). The experimental PXRD pattern of **1** is in good agreement with the simulated one from the single-crystal X-ray diffraction, demonstrating the phase purity of **1** (Fig. S3, ESI†).

The process of photocatalytic water oxidation under visible light illumination is shown in Scheme 1. A series of photocatalytic water oxidation experiments on compound **1** were carried out using an 80 mM borate buffer solution (initial pH = 9.0) with $[\text{Ru}(\text{bpy})_3]\text{Cl}_2$ as the photosensitizer and $\text{Na}_2\text{S}_2\text{O}_8$ as the sacrificial electron acceptor. Photocatalytic water oxidation reactions were carried out at different concentrations of catalyst **1** (0–10 μM , Fig. 2a) in 20 mL solutions.¹⁷ O_2 forms rapidly after irradiation and the amount of O_2 generated is quantified by online GC analyses. The total amount of generated O_2 increased as the catalyst concentration increased, whereas the O_2 evolution rate decreased sharply over time. The O_2 yields (O_2 yield = $2 \times$ mole of O_2 /mole of $\text{Na}_2\text{S}_2\text{O}_8$) increased from 5% to 17% with an increase in concentration of **1**. A maximum O_2 yield of 17% corresponded to the generation of 8.4 $\mu\text{mol O}_2$ when the concentration of **1** was 10 μM . Meanwhile, the turnover number (TON, defined as the mole of O_2 /mole of catalyst) decreased slightly from 51.2 to 42.2 with the catalyst concentration increasing from 2.5 to 10 μM . An initial turnover frequency (TOF, defined as the mole of O_2 /mole of catalyst/ Δt) in the first 300 s remains stable



Scheme 1 Compound **1** catalyzes water oxidation to generate O_2 under visible light irradiation, using $[\text{Ru}(\text{bpy})_3]^{2+}$ as the photosensitizer and $\text{S}_2\text{O}_8^{2-}$ as the sacrificial electron acceptor.

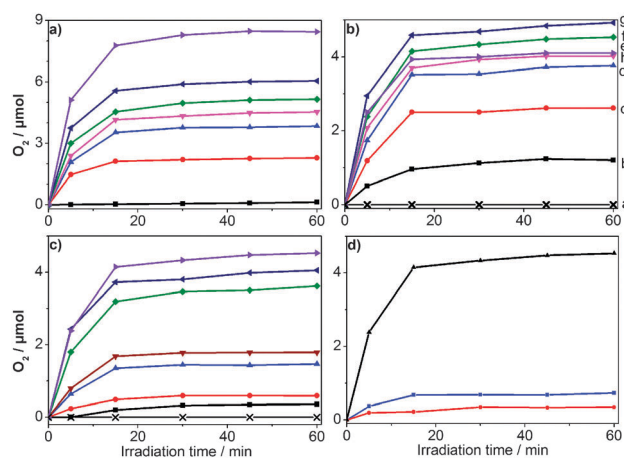


Fig. 2 Photochemical O_2 production from the borate buffer solution (80 mM, pH = 9.0). (a) 1.0 mM $[\text{Ru}(\text{bpy})_3]\text{Cl}_2$, 5.0 mM $\text{Na}_2\text{S}_2\text{O}_8$, and various concentrations of **1** (from bottom to top): 0, 2.5, 3.75, 5, 6.25, 7.5, and 10 μM . (b) 5 μM **1**, 1.0 mM $[\text{Ru}(\text{bpy})_3]\text{Cl}_2$, and various concentrations of $\text{Na}_2\text{S}_2\text{O}_8$: a, 0.0; b, 1.0; c, 2.0; d, 3.0; e, 4.0; f, 5.0; g, 6.0; h, 7.0 mM. (c) 5 μM **1**, 5.0 mM $\text{Na}_2\text{S}_2\text{O}_8$, and various concentrations of $[\text{Ru}(\text{bpy})_3]\text{Cl}_2$ (from bottom to top): 0.0, 0.1, 0.2, 0.4, 0.5, 0.8, 0.9, and 1.0 mM. (d) 1.0 mM $[\text{Ru}(\text{bpy})_3]\text{Cl}_2$, 5.0 mM $\text{Na}_2\text{S}_2\text{O}_8$, and a 1.76 μM mixture of $\text{Co}(\text{bpy})_3^{2+}$, $\text{Co}(\text{bpy})_2^{2+}$ and $\text{Co}(\text{bpy})^{2+}$ (red), 1.6 μM $\text{Co}(\text{NO}_3)_2$ (blue), or 5 μM **1** (black). Other conditions: a 300 W Xe lamp, 420–800 nm; total reaction volume of 20 mL; vigorous stirring (1.5×10^3 rpm).

between 0.08 and 0.10 s^{-1} with 10 μM **1**, indicating a 1st order kinetic dependence on the catalyst concentration. **The relatively low O_2 yield indicates that non- O_2 -evolving persulfate consumption reactions compete with the O_2 evolution process, which has been extensively studied earlier.**¹⁸ The competing non- O_2 -evolving persulfate consumption process can also be used to explain the observation that the O_2 total yield increases as the concentration of catalyst increases (Fig. 2a), since the desired O_2 evolution reaction is enhanced as the concentration of **1** increases. Without **1**, a maximum amount of only 0.12 $\mu\text{mol O}_2$ could be detected in 60 minutes under the same experimental conditions, substantiating the catalytic role of **1** in the water oxidation process.

The dependence of the O₂ generation rate on the concentrations of sacrificial electron acceptor Na₂S₂O₈ and photosensitizer [Ru(bpy)₃]Cl₂ was also examined systematically as shown in Fig. 2b and c. With an increase in the concentration of Na₂S₂O₈ from 1 to 6 mM, the total amount of O₂ evolution increased from 1.2 to 4.9 μmol, resulting in an increase in TON from 12.0 to 49.2. When the concentration of Na₂S₂O₈ further increased to 7 mM, however, only 4.1 μmol O₂ could be detected. Such an O₂ generation dependence on the Na₂S₂O₈ concentration was also observed in other POM systems.^{8b,d,18a} The O₂ yield decreased from 13% to 6% as the concentration of Na₂S₂O₈ increased from 1 to 7 mM. When the concentration of photosensitizer [Ru(bpy)₃]Cl₂ was below 1.0 mM, there was a positive correlation between the amount of evolved O₂ and the photosensitizer concentration. When the concentration of [Ru(bpy)₃]Cl₂ was varied from 0.1 to 1.0 mM, the O₂ yield increased from 0.7% to 9.1% and the TON increased from 3.52 to 45.32. No O₂ was detected in the absence of Na₂S₂O₈ or [Ru(bpy)₃]Cl₂. It should also be noted that there are six [Co(bpy)₃]²⁺ ions in each formula unit of **1**. The potential catalytic activity of [Co(bpy)₃]²⁺ was investigated by replacing **1** with [Co(bpy)₃](ClO₄)₂ (Fig. S4, ESI[†]). O₂ evolution was detected with a maximum amount of 0.22 μmol after 60 minutes of irradiation, corresponding to only 4.8% of the amount of O₂ generated in the presence of **1**. This result indicates that [Co(bpy)₃]²⁺ ions in **1** are not responsible for the observed water oxidation activity.

Under all of the tested conditions, the O₂ evolution saturates in about 15 min, consistent with the results seen for other POM-based WOCs.^{8d,18a} This phenomenon was explained by the complete consumption of Na₂S₂O₈ in this time period (due to non-O₂-evolving persulfate consumption processes).^{18a} Nevertheless, when we added another 5 mM of Na₂S₂O₈ (the same amount as the first round) to the system (5 μM **1**) after the catalysis, no more O₂ was generated upon irradiation. Similarly, no more O₂ generation was observed when we added either [Ru(bpy)₃]Cl₂ (1 mM, the same amount as the first round) alone or [Ru(bpy)₃]Cl₂ and Na₂S₂O₈ at the same time after the first round of catalysis. The O₂ generation did not recover even after the addition of the fresh POM catalyst into the system after the first round. In addition, after simultaneously adding all three components ([Ru(bpy)₃]Cl₂, Na₂S₂O₈, and fresh **1**) to the illuminated mixture after the first round of photocatalytic water oxidation and adjusting the pH to 9.0, still no oxygen could be detected after illumination for another hour. These results indicate that the catalyst is poisoned quickly during the first catalytic run. We also noticed that after completion of the first round (with 5 μM **1**, irradiated for 60 min), the pH of the buffer solution decreased from 8.92 to 8.52. To test the pH influence on the catalysis, we performed another photocatalytic experiment at a pH of 8.5 in borate buffer. The total amount of O₂ evolution was 1.5 μmol (33% of the pH 9.0 buffer under the same conditions, Fig. S5, ESI[†]). The decrease in pH is an important contributor to the loss of O₂ evolution activity after the first round.

Co²⁺ and CoO_x (form *in situ* from Co²⁺) in the aqueous solution are both known to be active WOCs.^{5a,19} The molecular WOCs also have the possibility of decomposing into catalytically active Co²⁺ or CoO_x. In the case of **1**, however, we have several

pieces of experimental evidence to rule out either Co²⁺ or CoO_x as the active catalyst in our system. Firstly, we performed extraction of the POM after photocatalysis.^{11b} The irradiated solution (80 mM pH 9.0 borate buffer containing 5 μM **1**, 1.0 mM [Ru(bpy)₃]Cl₂, and 5.0 mM Na₂S₂O₈, irradiated for 1 h) was treated by adding an excess amount of tetrabutylammonium bromide to extract the POM from the aqueous solution. Then, the amount of Co-containing species remaining in the aqueous solution was quantified by inductively coupled plasma-mass spectrometry (ICP-MS). Only 1.6 μM Co and 7.8 μM Mo were detected in the aqueous solution, indicating that less than 3.3% of **1** had decomposed. Moreover, the FT-IR spectrum of **1** extracted from the post-reaction solution shares the same pattern as the pristine sample of **1** (Fig. S6, Table S3, ESI[†]). Furthermore, **Dynamic Light Scattering (DLS)** experiments were performed on the reaction mixture before and after photocatalysis for **1**. A particle size of about 1.6 nm was determined for the solution of **1** both before and after the photocatalysis, corresponding to the size of the POM anion (Fig. S7a and b, ESI[†]). To ensure that the decomposed Co²⁺ or [Co(bpy)]²⁺/[Co(bpy)₂]²⁺ is not the dominant WOC species, we determined the WOC using 1.6 μM Co(NO₃)₂ or a 1.76 μM [Co(bpy)]²⁺/[Co(bpy)₂]²⁺/[Co(bpy)₃]²⁺ mixture²⁰ (the same amount as simple cobalt ions decomposed from 5 μM **1**). Only ~0.73 μmol O₂ was observed from 1.6 μM Co(NO₃)₂ and ~0.35 μmol O₂ from the 1.76 μM [Co(bpy)]²⁺/[Co(bpy)₂]²⁺/[Co(bpy)₃]²⁺ mixture, which accounts for 16.1% and 7.7% O₂ yield of **1**, respectively (Fig. 2d). **We also conducted a control experiment with a higher concentration of the [Co(bpy)]²⁺/[Co(bpy)₂]²⁺/[Co(bpy)₃]²⁺ mixture (contains 35 μM [Co(bpy)]²⁺ and [Co(bpy)₂]²⁺, the same amount of Co as that in 5 μM **1**).** The O₂ yield of the mixture is still lower than that of **1** (Fig. S8, ESI[†]). In contrast to **1**, formation of large nanoparticles of 60 nm/100 nm was observed by DLS in both control experiments with Co(NO₃)₂ and the [Co(bpy)]²⁺/[Co(bpy)₂]²⁺/[Co(bpy)₃]²⁺ mixture, indicating the formation of CoO_x in these cases (Fig. S7d and e, ESI[†]). With these experimental results, we conclude that the active WOC in **1** is unlikely to be a free cobalt ion or [Co(bpy)]²⁺/[Co(bpy)₂]²⁺ species formed from the decomposition of **1**.

The photocatalytic activity of **1** after aging for 5 h was also compared to that of the fresh catalyst (Fig. S9, ESI[†]). The amount of O₂ evolution did not change after the catalyst solution of **1** was left to stand for 5 h. We can infer that **1** is stable for at least 5 h under the catalytic conditions. The UV-Vis measurement of **1** also supports this conclusion: the absorption spectrum of the solution did not change after standing for 5 hours (Fig. S10, ESI[†]). We also performed cyclic voltammetry (CV) on **1** (Fig. S11, ESI[†]) which showed large, irreversible oxidative waves that correspond to catalytic water oxidation with an onset potential of ~0.98 V (vs. Ag/AgCl). From the results, we can conclude that oxidation of cobalt(II) in compound **1** to cobalt(III) species by [Ru(bpy)₃]³⁺ is thermodynamically feasible.

In conclusion, we have synthesized a novel bicapped/mono-capped Keggin-type POM (**1**) *via* a hydrothermal reaction and demonstrated the viability of **1** as a molecular water oxidation catalyst under photocatalytic conditions. The present WOC is built from the Keggin-type POM and bpy, two of the most robust building blocks for designing molecular WOCs. The photocatalytic

water oxidation activity of **1** has been studied systemically. A TON of up to 49 was observed, before the catalyst was poisoned by species generated during the catalytic process. The stability of **1** under photocatalytic conditions was demonstrated by DLS, extraction experiment, and UV-Vis and FT-IR spectroscopy. This work also demonstrates that POM clusters have the ability to enhance the WOC activity of bipyridine-substituted cobalt complexes and thus suggests new opportunities in designing hybrid molecular WOCs using POM and metal-bpy building blocks.

We thank the National Thousand Talents Program of P. R. China, the 985 Program of Chemistry and Chemical Engineering disciplines of Xiamen University and the US National Science Foundation (DMR-1308229) for funding support and Ms Ruiyun Huang for administrative help.

Notes and references

- (a) C. Starr, M. F. Searl and S. Alpert, *Science*, 1992, **256**, 981–987; (b) J. Chow, R. J. Kopp and P. R. Portney, *Science*, 2003, **302**, 1528–1531.
- (a) J. A. Turner, *Science*, 1999, **285**, 687–689; (b) Z. Şen, *Prog. Energy Combust. Sci.*, 2004, **30**, 367–416; (c) Z. Zou, J. Ye, K. Sayama and H. Arakawa, *Nature*, 2001, **414**, 625–627; (d) M. Grätzel, *Acc. Chem. Res.*, 2009, **42**, 1788–1798.
- (a) W. J. Youngblood, S.-H. A. Lee, Y. Kobayashi, E. A. Hernandez-Pagan, P. G. Hoertz, T. A. Moore, A. L. Moore, D. Gust and T. E. Mallouk, *J. Am. Chem. Soc.*, 2009, **131**, 926–927; (b) M. Yagi and M. Kaneko, *Chem. Rev.*, 2001, **101**, 21–36; (c) L. Duan, L. Wang, A. K. Inge, A. Fischer, X. Zou and L. Sun, *Inorg. Chem.*, 2013, **52**, 7844–7852; (d) L. Duan, L. Tong, Y. Xu and L. Sun, *Energy Environ. Sci.*, 2011, **4**, 3296–3313; (e) N. S. Lewis and D. G. Nocera, *Proc. Natl. Acad. Sci. U. S. A.*, 2006, **103**, 15729–15735; (f) J. H. Alstrum-Acevedo, M. K. Brennaman and T. J. Meyer, *Inorg. Chem.*, 2005, **44**, 6802–6827; (g) L. Duan, F. Bozoglian, S. Mandal, B. Stewart, T. Privalov, A. Llobet and L. Sun, *Nat. Chem.*, 2012, **4**, 418–423; (h) Y. Umena, K. Kawakami, J.-R. Shen and N. Kamiya, *Nature*, 2011, **473**, 55–60; (i) F. M. Toma, A. Sartorel, M. Iurlo, M. Carraro, P. Parris, C. Maccato, S. Rapino, B. R. Gonzalez, H. Amenitsch, T. Da Ros, L. Casalis, A. Goldoni, M. Marcaccio, G. Scorrano, G. Scoles, F. Paolucci, M. Prato and M. Bonchio, *Nat. Chem.*, 2010, **2**, 826–831.
- (a) S. M. Barnett, K. I. Goldberg and J. M. Mayer, *Nat. Chem.*, 2012, **4**, 498–502; (b) Z. Chen and T. J. Meyer, *Angew. Chem., Int. Ed.*, 2013, **52**, 700–703; (c) C.-F. Leung, S.-M. Ng, C.-C. Ko, W.-L. Man, J. Wu, L. Chen and T.-C. Lau, *Energy Environ. Sci.*, 2012, **5**, 7903; (d) G. C. Dismukes, R. Brimblecombe, G. A. N. Felton, R. S. Pryadun, J. E. Sheats, L. Spiccia and G. F. Swiegers, *Acc. Chem. Res.*, 2009, **42**, 1935–1943; (e) W. C. Ellis, N. D. McDaniel, S. Bernhard and T. J. Collins, *J. Am. Chem. Soc.*, 2010, **132**, 10990–10991; (f) J. L. Fillol, Z. Codolà, I. Garcia-Bosch, L. Gómez, J. J. Pla and M. Costas, *Nat. Chem.*, 2011, **3**, 807–813; (g) T. Zhang, C. Wang, S. Liu, J.-L. Wang and W. Lin, *J. Am. Chem. Soc.*, 2014, **136**, 273–281.
- (a) M. W. Kanan and D. G. Nocera, *Science*, 2008, **321**, 1072–1075; (b) F. Jiao and H. Frei, *Angew. Chem., Int. Ed.*, 2009, **48**, 1841–1844; (c) M. Zhang, M. de Respinis and H. Frei, *Nat. Chem.*, 2014, **6**, 362–367.
- (a) S. Bhaduri, M. Pink and G. Christou, *Chem. Commun.*, 2002, 2352–2353; (b) R. F. Bogucki, G. McLendon and A. E. Martell, *J. Am. Chem. Soc.*, 1976, **98**, 3202–3205; (c) A. J. Tasiopoulos, K. A. Abboud and G. Christou, *Chem. Commun.*, 2003, 580–581; (d) M. L. Rigsby, S. Mandal, W. Nam, L. C. Spencer, A. Llobet and S. S. Stahl, *Chem. Sci.*, 2012, **3**, 3058–3062.
- (a) D.-L. Long, R. Tsunashima and L. Cronin, *Angew. Chem., Int. Ed.*, 2010, **49**, 1736–1758; (b) H. N. Miras, J. Yan, D.-L. Long and L. Cronin, *Chem. Soc. Rev.*, 2012, **41**, 7403–7430.
- (a) H. Lv, Y. V. Geletii, C. Zhao, J. W. Vickers, G. Zhu, Z. Luo, J. Song, T. Lian, D. G. Musaev and C. L. Hill, *Chem. Soc. Rev.*, 2012, **41**, 7572–7589; (b) X.-B. Han, Z.-M. Zhang, T. Zhang, Y.-G. Li, W. Lin, W. You, Z.-M. Su and E.-B. Wang, *J. Am. Chem. Soc.*, 2014, **136**, 5359–5366; (c) Z. Han, A. M. Bond and C. Zhao, *Sci. China: Chem.*, 2011, **54**, 1877–1887; (d) F. Song, Y. Ding, B. Ma, C. Wang, Q. Wang, X. Du, S. Fu and J. Song, *Energy Environ. Sci.*, 2013, **6**, 1170–1184.
- Z. Huang, Z. Luo, Y. V. Geletii, J. W. Vickers, Q. Yin, D. Wu, Y. Hou, Y. Ding, J. Song, D. G. Musaev, C. L. Hill and T. Lian, *J. Am. Chem. Soc.*, 2011, **133**, 2068–2071.
- Q. Yin, J. M. Tan, C. Besson, Y. V. Geletii, D. G. Musaev, A. E. Kuznetsov, Z. Luo, K. I. Hardcastle and C. L. Hill, *Science*, 2010, **328**, 342–345.
- (a) J. J. Stracke and R. G. Finke, *ACS Catal.*, 2014, **4**, 79–89; (b) J. W. Vickers, H. Lv, J. M. Sumliner, G. Zhu, Z. Luo, D. G. Musaev, Y. V. Geletii and C. L. Hill, *J. Am. Chem. Soc.*, 2013, **135**, 14110–14118.
- G. Zhu, E. N. Glass, C. Zhao, H. Lv, J. W. Vickers, Y. V. Geletii, D. G. Musaev, J. Song and C. L. Hill, *Dalton Trans.*, 2012, **41**, 13043–13049.
- (a) F. Cavani, M. Koutyrev and F. Trifirò, *Catal. Today*, 1996, **28**, 319–333; (b) S. Kasztelan, E. Payen and J. B. Moffat, *J. Catal.*, 1990, **125**, 45–53.
- (a) A. K. Iyer and S. C. Peter, *Inorg. Chem.*, 2014, **53**, 653–660; (b) W. Liu and H. H. Thorp, *Inorg. Chem.*, 1993, **32**, 4102–4105; (c) R. M. Wood and G. J. Palenik, *Inorg. Chem.*, 1998, **37**, 4149–4151; (d) I. D. Brown and D. Altermatt, *Acta Crystallogr., Sect. B: Struct. Sci.*, 1985, **41**, 244–247.
- (a) J.-G. Choi and L. T. Thompson, *Appl. Surf. Sci.*, 1996, **93**, 143–149; (b) P. Gajardo, D. Pirotte, C. Defosse, P. Grange and B. Delmon, *J. Electron Spectrosc. Relat. Phenom.*, 1979, **17**, 121–135; (c) A. K. Iyer and S. C. Peter, *Inorg. Chem.*, 2014, **53**, 653–660.
- (a) J. P. Bonnelle, J. Grimblot and A. D’huysser, *J. Electron Spectrosc. Relat. Phenom.*, 1975, **7**, 151–162; (b) C. A. Strydom and H. J. Strydom, *Inorg. Chim. Acta*, 1989, **159**, 191–195.
- Each formula of **1** contains three bicapped Keggin structures and one monocapped Keggin structure. The catalytic activity based on the Co^{II}bpy unit is likely 7 times lower than the value that is calculated based on the formula of **1**.
- (a) S. Tanaka, M. Annaka and K. Sakai, *Chem. Commun.*, 2012, **48**, 1653–1655; (b) K. Henbest, P. Douglas, M. S. Garley and A. Mills, *J. Photochem. Photobiol., A*, 1994, **80**, 299–305; (c) A. B. Tossi and H. Görner, *J. Photochem. Photobiol., B*, 1993, **17**, 115–125.
- (a) A. Harriman, I. J. Pickering, J. M. Thomas and P. A. Christensen, *J. Chem. Soc., Faraday Trans. 1*, 1988, 2795–2806; (b) P. K. Ghosh, B. S. Brunschwig, M. Chou, C. Creutz and N. Sutin, *J. Am. Chem. Soc.*, 1984, **106**, 4772–4783.
- The [Co(bpy)₃]²⁺: [Co(bpy)₂]²⁺: [Co(bpy)]²⁺ (1:9:1, 1.76 μM total Co concentration) mixture contains 1.6 μM [Co(bpy)]²⁺ and [Co(bpy)₂]²⁺. [Co(bpy)₃]²⁺ is known to be an inactive WOC. See ESI† for more details.